REPUBLIQUE ALGERIENNE DEMOCRATIQUE ET POPULAIRE
الجمهورية الجزائرية الديمقراطية الشعبية

MINISTERE DE L'ENSEIGNEMENT SUPERIEUR ET DE LA RECHERCHE SCIENTIFIQUE

ECOLE SUPERIEURE EN SCIENCES APPLIQUEES
--T L E M C E N--

وزارة التعليم العالي والبحث العلمي

المدرسة العليا في العلوم التطبيقية
-تلمسان-

End-Of-Study manuscript

To obtain the Master degree

Branch : Electrical engineering
Speciality: Energy and Environnement
Presented by: SAOUD ROUMAISSA

Theme

Optimizing the magnetic heat exchangers of thermomagnetic motors: A heat transfer study

Presented, on 29 / 09 / 2021, Infront of the committee:

Mr F. Maliki	MCB	ESSA. Tlemcen	Commitee President
Ms A. GHOMRI	Pr	Univ. Tlemcen	Spervisor
Mr N. DAHMANI	MCA	UNIV. Tlemcen	Examiner 1
Ms A. CHIALLI	MCB	ESSA. Tlemcen	Examiner 2

University year : 2020/2021

"Success is not final, failure is not fatal: It is the courage to continue that counts."

-- Winston S. Churchill

Dedecace

To my mother, I want her to know how much I love her and how proud I am of her. She is my role model, I admire her strength and courage in dealing with her illness. My mum means everything to me, I don 't tell her enough that I love her and I regret it. I hope one day to be like her, my mum I love you.

To my father, my oncles Mohammed, Ilyes , Abd-elkadder for being here always with me in every step on my way.

To my brothers Ahmed-Ayoub ans Anes wish u all the best my little bros

To my cousins Sabrina, Radia, Amina, Anissa, Younes and Nadjet for sopporing me

To my dear friends my sisters and brothers :
Kaouthar, Hayet, Ghizlene, Keltoum, Wissem, Aya, Yamina, Meriem Abdessalem Hocine,, Sofiane, Louai, Nasreddine, Mounir for giving me the support that I needed this year to finish this work without you I could not finish thanx a lot for all your advices, encouragement, thank you for being there when I really needed you especially this year which really marked me, I could not be here without your support

To my family the Texquad family my club my home my everything love you my sons and daughters

Roumaissa

Acknowledgements

Researching, executing, and compiling this report was a very challenging and rewarding experience for me.

I have gained rich knowledge and, valuable experience through my thesis work. Although this is presented as our work, we could not have completed it without the help of God.

So, first and above all, I praise our God and lord, the almighty for providing me with all of the strength, courage and success throughout my education journey and especially through this hard period of time.
Thank you, god, for allowing me to finish my journey and for giving me the ability to write this thesis. Apart from our efforts, this thesis' success depends largely on the motivation and guidelines of many others.

I would like to make this an opportunity to express our gratitude to the people who have been influential in the successful completion of this thesis.

I would like to express our deepest appreciation to my mother, my life mentors, strong women who has been through a lot and yet stood still, always encouraging, supporting and leading me to the success path with her valuable advices, patience, precious time and hard work spent in my favor.

I am deeply indebted to my father, who always trusted us in every step I took, who never gives up on me, worked hard for my sake and gifted us with his eternal love.

I extend my sincere thanks to our supervisors, Misses Amina GHOMRI a professor and MCA,and Mr.Abderrezak SOUID head of engineering division at SONATRACH for giving me the opportunity to work with them, I admire ther guidance, decision-making skills, orientation and of course the trust sthey gave us throughout the whole working process.

This journey would not have been possible without, our teachers and course instructors, our school, the superior school of applied science and its academic stuff; fellow classmates with whom we spent 5 years filled with beautiful memories, fun moments of laughter and joy, and from whom we have learned plenty of lessons.

Thank you for all of you and every one of you. Finally, special thanks to Mr. Maliki Fouad, head of department of industrial engineering speciality, a professor and MAA at the Superior school of applied science, Tlemcen; to Mr. Chialli Aniss, the responsible of the exterior relations, a professor and MCB at the Superior school of applied science, Tlemcen; to Misses N,DAHMANI MCA at ABB University , Tlemcen for taking some of their busy and precious time to discuss and enrich our work

Table of Contents

Table des matières

List of figures

List of tables

List of abbreviations and acronyms

- b width of the magnetic rotor/ the armature m
- **B** magnetic flux density, induction . . . . . $V \cdot s \cdot m^{-2}$
- B_A flux density in the gap . . . . . $V \cdot s \cdot m^{-2}$
- BS saturation flux density . . . . . $V \cdot s \cdot m^{-2}$
- B_{Smax} maximum saturation flux density . . . . $V \cdot s \cdot m^{-2}$
- d thickness of the rotor . . . . . m en unit vecto
- F force . . . . . N
- F_m magnetic force . . . . . N
- g heat generation rate . . . . . $W \cdot m^{-3}$
- **H** magnetic field strength . . . . . $A \cdot m^{-1}$
- k thermal coductivity . . . . . $W \cdot m^{-1} \cdot K^{-1}$
- M module in the explicit difference method
- N magnetic North Pole
- q heat flux . . . . . $W \cdot m^{-2}$
- S magnetic South Pole
- s distance . . . . . m
- s_A length of the rotor in the gap . . . . . m
- t time . . . . . s
- T thermodynamic temperature . . . . . K
- V volume . . . . . m^3
- W_m energy of the magnetic field . . . . . J
- w_m energy density of the magnetic field . . . $J \cdot m^{-3}$
- v velocity . . . . . $mm \cdot s^{-1}$
- x coordinate
- P power . . . . . W
- **Greek symbols**

- α absorptivity; thermal diffusivity . . . . . $m^2 \cdot s^{-1}$
- x section size in x-direction . . . . . m
- Θ temperature . . . . . °C
- ϑ_A temperature of the armature/rotor . . . . °C
- ϑ_C Curie temperature . . . . . °C
- ϑ_U ambient temperature . . . . . °C
- η_{therm} thermal efficiency
- η_{ex} exergetic efficiency

General Introduction

General Introduction

The concept of sustainable development has been widely discussed in the past few decades. According to the report of the World Commission on Environment and Development (WCED, 1987) [1], Sustainable development is the answer to the problems brought about by traditional development. Traditional development only focuses on economic growth, while changes in other parts of society are only a result. Today, the term sustainable development is closely related to the term sustainability. Sustainability mainly refers to ecological issues (the relationship between biological organisms and their environment). As Baker believes, its roots are that “the main focus of sustainable development is society".

She further explained that sustainable development refers to the coordination of social changes between the social, economic and ecological aspects representing the three pillars of sustainable development. The entire concept of sustainable development is oriented towards the future, as the UN’s definition of this concept pointed out: "Sustainable development is the development of meeting the needs of the present without compromising the ability of future generations to meet their needs."

Or, as Baker argues, sustainable development is about imagining alternative futures and adopting one that is sustainable. In other words, sustainable development is about developing different sets of future scenarios and doing its best to implement the most preferred one. For the concept of sustainable development (or lifestyle) to become widely accepted, people need a shared understanding of the future, good and bad.

The path to understanding is by visualizing abstract concepts and communicating them not only to the scientific community, but to society as a whole. In this sense, the report puts forward the fact that energy is necessary for daily survival. The key to future development depends on its increasing long-term availability from reliable, safe and environmentally sound sources.

Energy demand in the world is nowadays growing further out of limits of installable generation capacity.[1]

Therefore, future energy demand should be met and improved efficiently and safely. Energy solutions should be supported by the use of renewable energy sources. Currently, the contribution of renewable energy to the world's primary energy is not high to cover the supply of primary energy and electricity. Both developed and developing countries will by necessity continue to rely on fossil fuels for decades to come. In developing countries, the situation is more uncomfortable than in developed countries. Many developing countries have apparently tried to restructure their energy

sectors. It seems difficult to innovate. Costs, market share and policy are the main barriers to the development of renewable energy. In the strategic plans of many countries, sustainable development in relation to parameters such as economic, social and industrial is supported by their energy policy.

New enabling technologies related to renewable energy will also reduce environmental costs, and thus energy systems will be operated both safely and economically, without environmental problems. New renewable energy markets are certainly needed in both the wholesale and retail markets. To resume currently, there is no single source or mixed source at hand to meet this future demand.

The magnetic conversion system can represent an alternative to producing energy in a cleaner and more sustainable way. This technology can be traced back to the 19th century, when many scientists including Tesla and Edison filed a patent for the so-called “pyro-magnetic generators”. When Tesla and Edison submitted their patents permanent magnets were not strong enough, nor were the appropriate magnetic materials available to build economical and practical devices. Several proposals of thermomagnetic devices to convert thermal energy into mechanical or electrical energy are found in the literature. In 1959 Elliot did analysis of a thermomagnetic generator without moving parts, Merkl proposed a kind of thermomagnetic step-motor (Merkl, 1969), in 1972 Murakami proposed and analyzed a thermo-magnetic motor for work with hot sources with temperatures around room temperature (Murakami and Nemoto, 1972), and the same has been done by Karle (2000) and Takahashi et al. (2004, 2006). Recently, Xuan described a cooling system for electronic devices using Ferro fluids (Xuan and Lian, 2011), and Trapanese et al. designed a Gd-based thermomagnetic motor.

The power produced by a motor is proportional to the product between its torques or force times its operational frequency or velocity. In thermomagnetic motors the torque or force produced depends mainly on the magnetic energy stored in the air gap between the magneto-caloric material plates and the permanent magnet arrangement (Halbach, 1980); therefore obtaining high torques or forces in thermomagnetic motors isn’t something of a challenge. However, the great drawback of this technology is the low frequencies produced by these kinds of motors, since the process of heating up a material is slow, so that the anticipated dynamics does not allow the speeds typical of electrical motors (Karle, 2000). In this sense, the frequency produced by thermomagnetic motors is a direct result of the heat transfer rate between the magneto-caloric material and the working fluids.

Our study is structured as follows: in the first part we proceed to General information on heat exchangers. A second chapter is reserved for the detailed description of Curie-Motor. The third chapter contains the results the optimization of curie motor.

Chapter I: general information on heat exchangers

1.1. Basic concepts

A heat exchanger is a piece of equipment that allows heat to be transferred from a hot fluid to a cold fluid without direct contact between the two fluids. The same fluid can remain in its physical state (liquid or gas) or be in both phases in succession: this is the case of condensers, evaporators, boilers or cooling towers .[2]

In principle, for the most common heat exchangers in industry, the two fluids flow in spaces separated by a wall or partition with low thermal inertia through which the exchanges take place by conduction. In fact, the heat that one of the fluids gives up to the wall by convection along the contact surface is transferred by conduction and is given up to the other fluid by convection along the other face. Radiation only plays a significant role if there are very large temperature differences between a fluid and the wall.

1.1.1. Heat transfer coefficients

Heat exchanges by convection, whether forced or natural, are the consequence of fluid movements caused respectively by an external action or by the difference in density between the hot and cold parts of the fluid [2]. The concept of transfer coefficient is based on the proportionality between the flows exchanged between the phases and the differences in their temperatures [3].
Thus, the surface density of heat flux convicted between two solid and fluid phases at two different average temperatures is written according to Newton's law as:

$$\Phi_{conv} = h\,(T_s - T_f) \qquad (1.1)$$

The exchange coefficient h ($W.m^{-2}.K^{-1}$), translates empirically the heat exchange of the solid with the fluid, it represents a conductance by analogy with heat transfer by conduction. Indeed, in the case of a homogeneous and isotropic plane wall, of thickness and thermal conductivity λ_{wall} whose two faces are subjected respectively to the

At temperatures T_e and Ts, the heat flux density is written according to Fourier's law such that:

$$\phi_{cond} = \frac{\lambda_w}{e} (T_s - T_e)$$

On the other hand, by assimilating the temperature profile to a straight line in the thermal boundary layer that develops when a fluid flow rubs against a solid wall, the convicted flux density can also be written:

$$\phi_{conv} = h.(T_S - T_f) = \frac{\lambda_{gaz}}{\delta_{th}} (T_s - T_f) \qquad (1.2)$$

This notion of convective exchange coefficient is very controversial. Indeed, it should be noted that the considerations concerning this exchange coefficient are only valid in the steady state. Generally, the values of the exchange coefficient h depend on the hydrodynamic and thermal conditions of the fluid phase in presence:

- Viscosity
- Conductivity
- Heat density
- Flow velocity
- Temperature…etc.

In the unsteady regime, heat transfer inertia effects have to be taken into account in the fluid, and cannot be considered as simply. Indeed, the exchange coefficient is not an intrinsic characteristic of the boundary layer since it depends on the nature of the thermal boundary conditions. It is thus a convenient but not totally meaningful quantity from the physical point of view.

1.1.2. Heat transfer in dimensionless form

When the fluid is in forced flow, the universal form writing of the convection correlations involves three dimensionless groupings:

- The Nusselt number which represents the ratio between the heat fluxes transmittedby convection and by conduction:

$$NU=\frac{hL}{\lambda_{gas}} \qquad (1.3)$$

Where L is the characteristic quantity of the system, λ_{gas} the thermal conductivity of the gas in presence and h the local or global exchange coefficient according to the cases considered.

- The Reynolds number which reflects, on the one hand, the competition betweenconvection and diffusion, and on the other hand, the type of fluid flow:

$$Re = \frac{Lu}{v} = \frac{\rho Lu}{\mu} \qquad (1.4)$$

Where L and u represent the characteristic length and velocity of the flow, and ρ, ν and μ represent the density, kinematic viscosity and dynamic viscosity of the fluid, respectively.

- The Prandtl number which characterizes the relative importance of thermal andviscous effects of a fluid in a given state:

$$Pr = \frac{v}{\alpha} = \frac{\mu c_p}{\lambda_{gas}} \qquad (1.5)$$

The heat transfer coefficient, expressed as the Nusselt number, is usually expressed as a function of the Reynolds number and the Prandtl number:

$$Nu = f(Re,Pr) \qquad (1.6)$$

Regardless of the flow regime, a multitude of empirical or semi-empirical relationships existin the literature to express the Nusselt number.

1.2. Classification and flow mode

Due to their different applications, the characteristics of heat exchangers fall within a very wide range, in terms of exchanged power, pressure and temperature. The operating requirements, the different standards imposed by the legislator for the design of such devices, the technologies as well as the materials used are inevitably varied and difficult to compare.

It is therefore difficult to establish a rigorous classification without making the undeniably restrictive choice of a criterion. Most often, heat exchangers are classified according to the flow configuration of the fluids considered and according to their type of construction.

1.2.1. Main flow modes of the two fluids

Three different flow modes can be distinguished; Flow of two fluids parallel and in the same direction.

These are so-called co-current exchangers where the temperature of the cold fluid cannot be higher than the outlet temperature of the hot fluid. The temperatures of the fluidschange during their longitudinal passage through the exchanger, unless one of the fluids undergoes a phase change, in which case its temperature remains constant.

Figure 1.1 shows the qualitative evolution of these temperatures along a very simple co- current tube exchanger. The length of the exchanger has been plotted on the abscissa **[2-3].** The temperatures are marked with indices "e" meaning inlet and "s" outlet,"1" designates the hot fluid and "2" the cold fluid.

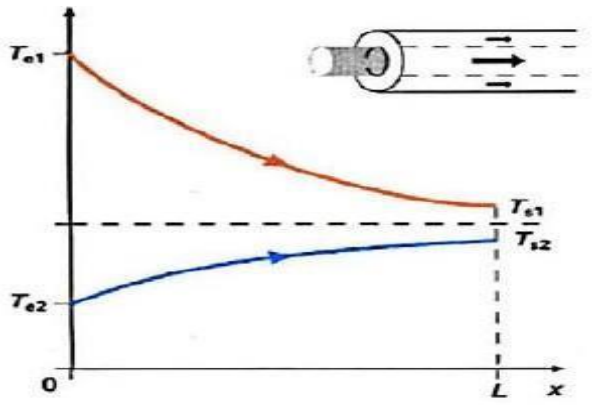

Figure 1.1.qualitative temperature evolution in a co-current shell-and-tube exchanger [4]

1.2.2. Flow of two fluids parallel but in opposite directions

These are countercurrent exchangers where the outlet temperature of the cold fluid can exceed the outlet temperature of the hot fluid. This arrangement is the most favourable for heat exchange. In the same way as before, the length of the exchanger considered has been plotted on the abscissa. The temperatures are marked with the subscripts "e" for inlet and "s" for outlet **[5,6].**

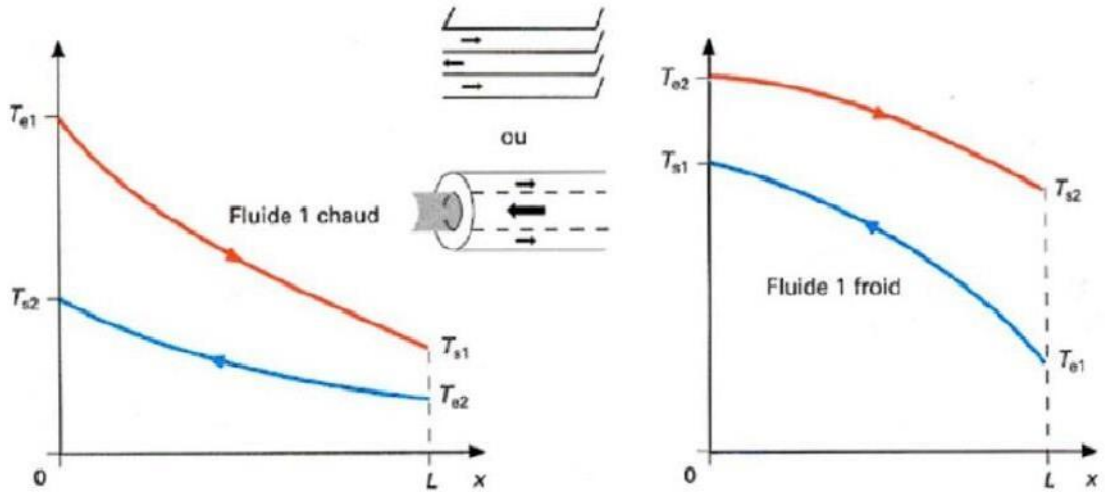

Figure 1.2: qualitative temperature evolution in a counter flow tube or plate heat exchanger [4]

The advantage of the countercurrent exchanger over the co-current exchanger is that smaller exchange surfaces are required for the same heat flow.

1.2.3. Cross-flow of two fluids with or without mixing

The two fluids flow perpendicular to each other (Figure 1.3). The unmixed fluid is channelled: it is the one whose vein is divided between several distinct parallel channels of small section. The other fluid flows freely between the veins and can be considered as partially stirred because of the vortices generated by the tubes. The stirring has the effect of homogenizing the temperatures in the straight sections of the fluid stream. Without this, the temperatures vary not only with the direction of the flow, but also in the cross-section of the flow; a schematic representation of crossflow heat exchangers is given (Figure 1.3).

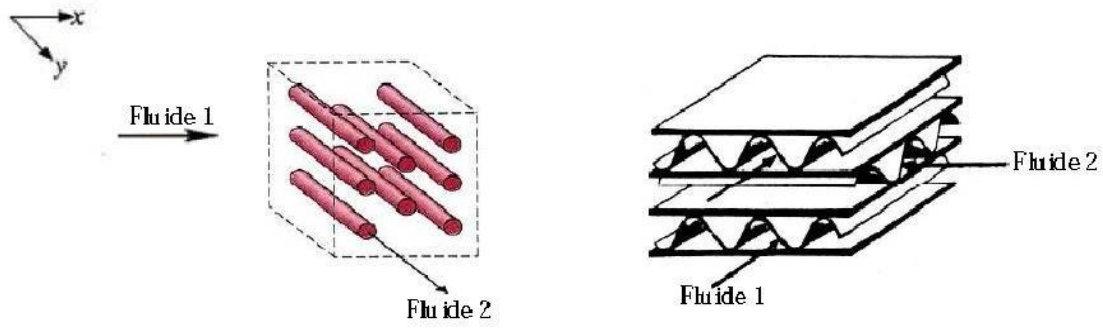

Figure 1.3: exemples of cross-flow exchangers [4]

The three flows described above, co-current, counter-current and cross-current, arerarely used in all their simplicity. Indeed, an exchanger is rarely reduced to a single tube or two plates; nevertheless, the study of these elementary cases, as a first approach, is necessary: the industrial exchanger being in general constituted by a great number of tubes or plates thus creating additional problems. Moreover, the design of heat exchangers introduces the choice between two main elementary geometries:

- The tubes that fix the space dedicated to only one of the two fluids.
- The plates, flat or corrugated, chosen for one fluid which impose the samegeometry

For the others, often the choice of combinations between the uses of different types of heat exchangers in industrial plants is the result oftechnological and economic contingencies.

1.3. Classification of exchangers

Heat exchangers can be classified in many different ways [7]**,** so in the following we will only mention the groups that we consider important.

- Classification according to their heat transfer processes heat exchangers are classified into two types: direct contact and indirect contact.
- Classification according to surface compactness. This other classification, which is arbitrary, is based on the ratio of the exchange surface area to the volume of the exchanger and is divided into two categories: compact and non-compact exchangers.
- Classification according to construction Tubular heat exchangers: coaxial, multi-tube, tube and shell, double tube coaxial and shell.
- Classification according to the nature of the material of the exchange wall:

    1. Metallic exchangers: steel, copper, aluminium...
    2. Non-metallic exchangers: plastic, ceramic, etc.

- Classification according to the number of fluids
- Classification according to flow direction
- Classification according to the heat transfer mechanism

1.3.1. Tubular exchangers:

Heat exchangers using tubes as the main component of the exchange wall are the most widespread. Three categories can be distinguished according to the number of tubes and their arrangement [4]**,** always designed to have the best possible efficiency for a given use:

1.3.2. Single pipe exchanger

In this heat exchanger the tube is placed inside a tank and is usually shaped like a coil (Figure 1.4).

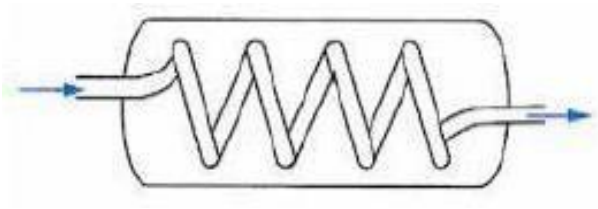

Figure 1.4 monotube exchanger [4]

1.3.3. Coaxial exchanger

In this heat, the double tubes are the most often curved; inIn general, the hot or high-pressure fluid flows through the inner tube (Figure 1.5).

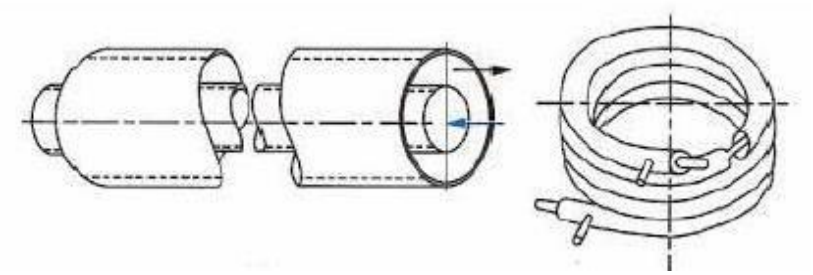

Figure 1.5 Curved coaxial exchanger [4]

1.3.4. Multi-tube exchanger

1.3.4.1. Separate tube exchanger

Inside a tube of sufficient diameter (around 100 mm) are several small diameter tubes (8 to 20 mm) held apart by spacers. The exchanger can be either straight or coiled (Figure 1.6).

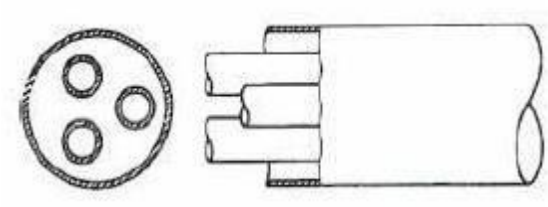

Figure 1.6 Separate tube exchanger [4]

1.3.4.2. Tube and shell heat exchangers

The main tube and shell heat exchanger technologies are shown in (Figure 1.7); the fouling and the temperature between the two technologies are two parameters that differentiate the main.

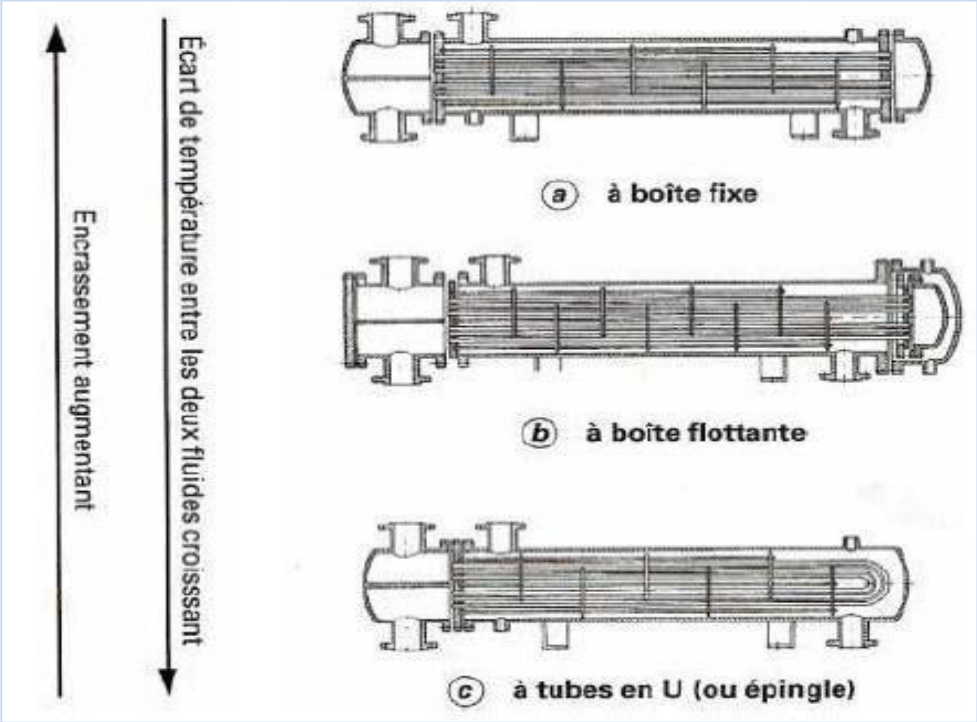

Figure 1.7. Main technologies of shell and tube heat exchangers [4]

1.3.5. Heat exchanger with double concentric tubes and shell

The new heat exchangers [8] are similar to the conventional heat exchangers mentioned below, the difference being that the single or corrugated tubes with or without fins, are now replaced by double coaxial tubes (double shell tubes). The outer diameter of the shell of the concentric double tubes is of the same order as the tubes used in conventional shell and tube heat exchangers.

Mainly, the second tube improves the heat transfer by a section ofand a larger heat transfer surface per unit of capacity.

Length of the heat exchanger also, two new tube plates are added to hold and distribute a fluid in the inner tubes of the double tubes

(Figure 1.11) The two old tube sheets are still used For holding and distributing the fluid passing through the annular passage formed by The two concentric tubes so instead of the heat exchanger working with two fluids (one hot and one cold fluid), now the heat exchanger works with three fluids (2 hot fluids and one cold fluid C-F-C or the opposite F-C-F). The fluids can be of the same nature or not.

In the double tube concentric shell and tube heat exchanger shown in figures (1.8, 1.9, 1.10), we see the shell, the 3 distributors, the 3 manifolds, the distribution boxes and the outside of the four tube plates. The two fluids of the same temperature level enter through the first and third distributor and exit through the third and first manifold respectively. The fluid with a different temperature level than the other two fluids always enters and exits through the adjoining manifold (distributor).

The first fluid (same temperature level or nature as the third fluid) enters through the first distributor and passes through the first tube sheet and exits through the fourth tube sheet and the last header as shown in (Figure 1.8). While the second fluid enters the heat exchanger through the second distributor and passes through the ring-shaped passages formed by the inner tubes and the second tube sheet and then leaves the exchanger through the third tube sheet (see Figure 1.8) and the second to last manifold (see Figure 1.8). The third fluid enters the exchanger through the third distributor and crosses the exchanger on the outer side of the double shells (shell side) and leaves the heat exchanger through the first manifold in the same way as the conventional shell and tube exchangers (Figure 1.8).

These double tube concentric and shell and tube heat exchangers are constructed in different ways, depending on the condition of the fluids present. The tubes can be fined or corrugated. Generally, the fluid circulating on the calendar side can circulate at multipass due to the presence of baffles. This allows a better irrigation of all the tubes. The baffles are plates with holes of different shapes: segments, discs, circular holes, circular trunks, etc. The tubes can be arranged in the bundle in an aligned or staggered arrangement, see (Figure 1.10).

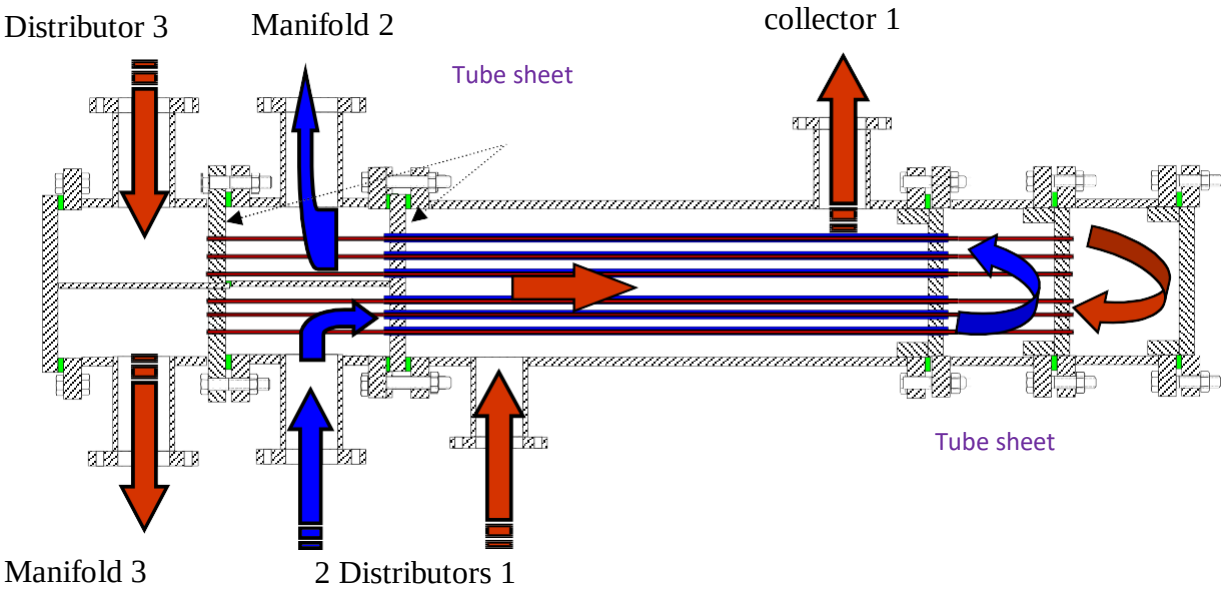

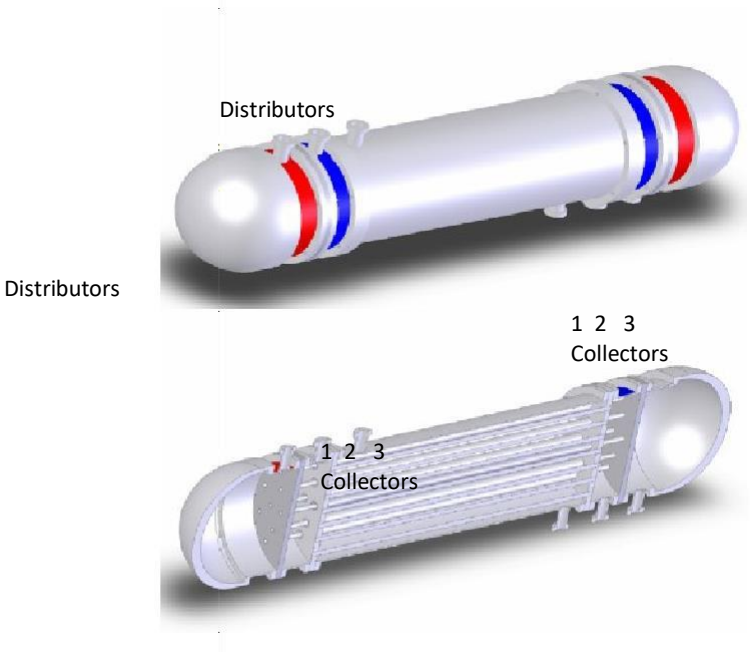

Figure 1.8. Perspective view and longitudinal section of the double concentric tubeexchanger and shell

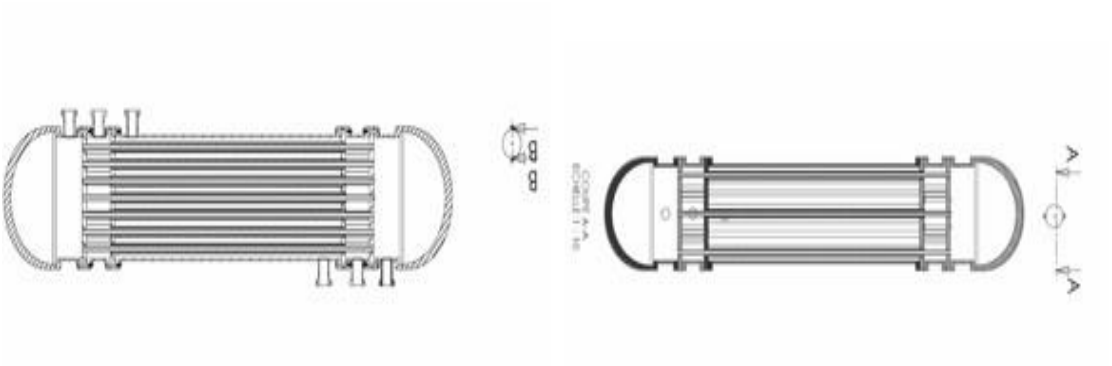

Figure 1.9. Cross-section A-A and B-B of the double tube concentric heat exchanger and shell

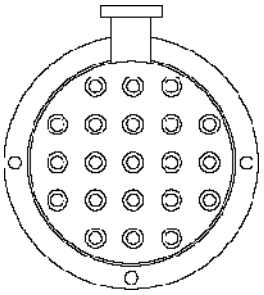

Figure 1.10. Cross-section of the heat exchanger along the C-C direction

Figure 1.11. Tube plate for double tubes

1.3.5.1. Method of realization

The construction of the double tube concentric heat exchanger and shell is similar to that of the tube and shell. The only change is that the double concentric tubes are mounted on two tube plates at each end of the heat exchanger.

The first tube plate has holes with a diameter equal to the inner diameter of the inner tube of the double shell while the second tube plate has holes with a diameter equal to the inner diameter of the concentric double tube shell.

The first plate and the second plate (or the third and fourth plates) are separated by a cylindrical trunk to which the manifold (or distributor) of the second fluid is welded.

1.4. Selection criteria and requirements

1.4.1. Selection criteria

There are many selection criteria, but the main ones are the nature of the fluid to be treated, the operating pressures and temperatures, and the costs.

The fluids involved in heat transfer can be characterized by temperature, pressure, phase, physical properties, toxicity, corrosivity, and tendency to fouling. The operating conditionsof heat exchangers vary in a very wide range, and a wide range of requirements is imposed for their design and performance [7]**.**

All of these elements must be considered when evaluating the type of heat exchanger to be used. When selecting a heat exchanger for a given task, the following points should be considered:

1. Building materials
2. Operating pressure and temperature,
3. Flow rates
4. Type of flow
5. Performance parameters: Thermal efficiency and pressure drop
6. Danger of clogging
7. Types and phases of fluids

8. Maintenance, inspection, cleaning, extension and repair possibilities
9. Overall cost
10. Manufacturing techniques
11. Applications for

1.4.2. Selection requirements

Heat exchangers must meet the following requirements**:**

1. High thermal efficiency
2. Lowest possible pressure loss
3. Reliability and life expectancy
4. High quality product and safe operation
5. Compatibility of materials with operating fluids
6. Convenient size, easy to install, reliable to use
7. Easy to maintain and repair
8. Lightweight yet robust in construction to withstand operationalpressures
9. Simplicity of manufacture
10. Low cost
11. Possibility of repairing maintenance problems

1.5. Literature review

The shell and tube heat exchanger is a classic heat exchanger, but the variety of models available, the specifications that must be met and the large number of variables that must be calculated can make its sizing a very complex operation. Currently, research is focused on the use of advanced optimization techniques for the sizing of heat exchangers.

In the following, the most important studies on the sizing of shell and tube heat exchangers using optimization techniques and especially the genetic algorithm method are mentioned.

Resat S, Onder K, Marcus R [9]**,** applied the genetic algorithm for the optimal design of the shell and tube heat exchanger by varying the design variables: tube outer diameter, tube arrangement, number of tube passes, shell diameter, baffle gap and baffle cut. The authors show the successful application of the genetic algorithm for the optimal design of the shell and tube heat exchanger. They concluded that combinatorial algorithms such as the genetic algorithm can provide a significant improvement in optimization compared to traditional design methods. The application of the genetic algorithm determines the minimum overall cost of the heat exchanger significantly faster and has an advantage over other methods in obtaining multiple solutions of equal quality. Thus, it provides greater flexibility to the designer.

M. Fesanghary, E. Damangir a, I. Soleimani [10], used global sensitivity analysis (GSA) and harmonic search algorithm (HSA) for the design optimization of shell-and-tube heat exchanger from the economic point of view, the design variables are chosen using global sensitivity analysis (GSA) which allows to discard the geometrical parameters that have little influence on the overall cost of the exchanger and reduces the size of the optimization problem. To demonstrate the efficiency and accuracy of the proposed algorithm, an illustrative example is studied. Comparing the results of HSA with those obtained using the Genetic Algorithm (GA) reveals that HSA can converge to an optimal solution with more accuracy.

André L.H. Costa, Eduardo M. Queiroz [11]**,** optimized the design of shell and tube heat exchangers by minimizing the heat exchange surface for a certain service, involving discrete decision variables: external diameter of the tubes, internal diameter of the tubes, total number of tubes, length of the tubes, number of passes, space between baffles, cross- section of baffles.

The optimization algorithm is based on a search along the calculation table where the established constraints and the design variables of the studied case are used to eliminate the non-optimal alternatives, thus reducing the calculation time.

The performance of the algorithm and its individual components are explored through two design examples; the obtained results illustrate the ability of the proposed modeling to direct the optimization towards more efficient designs, taking into account constraints generally ignored in the literature.

Sepehr Sanaye, Hassan Hajabdollahi [12], optimized the tube and shell heat exchanger in multi-objective by studying two objective functions, maximizing the efficiency and minimizing the total cost, which is the sum of investment cost (exchange area) and operating cost (power required to overcome the pressure drops). The design variables are: tube arrangement, tube diameter, distance between baffles, baffle cut, number of tubes, tube length. Thermal modeling based on Ɛ-NUT method was applied to calculate the convective heat transfer coefficient and pressure drop calculation. The optimization technique used is Genetic Algorithm to maximize the efficiency and minimize the total cost at the same time.
The results found are a series of optimal solutions called Pareto optimal solutions and to show the importance of each design variable on the optimal design of the shell and tube heat exchanger a sensitivity analysis of each variable was done.

Arzu Sencan Sahin, Bayram Kılıc, Ulas Kılıc [13], used the Artificial Bee Colony (ABC) method to optimize the design of the tube-and-calender heat exchanger to minimize the total equipment cost, including the capital cost and the sum of the present value of the annual energy costs of pumping the shell and tube heat exchanger by varying the different design variables such as tube length, tube outside diameter, pitch size, baffle spacing, ...etc.

The obtained results are compared with those in the literature. The obtained results indicate that the Artificial Bee Colony (ABC) algorithm can be successfully applied for the optimal design of the shell and tube heat exchanger.

Dogan Eryener [14], finds that despite the importance of thermos-economic analysis of the shell and tube heat exchanger design, the determination of the optimal baffle spacing using thermos-economic analysis is generally neglected in the literature. On the other hand, the baffle spacing is one of the most important parameters used in the design of shell and tube heat exchangers.

He used thermo-economic analysis to determine the optimum baffle spacing in the design of the shell-and-tube heat exchanger, and provided an example of such a baffle spacing

optimization. He used thermo-economic analysis to determine the optimal baffle spacing for the shell and tube heat exchanger design, along with an example of such a baffle spacing optimization for a shell and tube heat exchanger. The results of this example are then used to demonstrate how the optimal ratio of baffle space to shell diameter is accurately determined and affected by the different values of the geometric parameters. Finally, the results are compared to those obtained by conventional simulations.

Fettaka S, Thibault J[15], Gupta Y used multi-objective optimization by genetic algorithm method to minimize the pumping capacity and heat transfer area for a shell and tube heat exchanger, the design variables are: tube thickness, number of tubes per pass, number of pass, distance between baffles, baffle cut, tube length, arrangement, tube outer diameter. They determined the effects of using continuous values of tube thickness, length and diameter on the optimum pumping and heat transfer performance.

Ponce-Ortega JM, Serna-Gonzalez M, Jimenez-Gutierrez A [16] used the Bell-Delaware method for the description of the shell side flow without simplifications in a genetic algorithm for the optimal design of shell and tube heat exchangers. The selected decision variables were: standard inner and outer tube diameters, number of tubes per pass, head type, fluid distribution and number of sealing strips. They conclude that genetic algorithms provide a valuable tool for the optimal design of heat exchangers. Genetic algorithms and entropy generation minimization method are used by Huang [17] to optimize the design of heat exchangers. The results also demonstrated their effectiveness and feasibility of use.

Antonio C, Pacifico M. Pelagagge, Paolo Salini [18], have given a method for solvingthe optimization problem of shell and tube heat exchanger design based on the use of a genetic algorithm. It reduces the total cost of the equipment, including the capital cost and the operating cost related to the annual pumping energy costs. In order to verify the capability of the proposed method, three cases are presented showing that significant cost reductions are feasible with respect to the traditional exchanger design. In particular, in the cases examined a reduction in total costs of over 50% was observed

Mansouri Larbi, Mourad Balistrou, Bernard Baudoin [19], have numerically studied the stationary laminar forced convection in the dynamic regime established in the inlet zone of a tubular heat exchanger. They assumed that the heat transfer in the exchanger is without thermal losses, two-dimensional (axisymmetric) in stationary regime. The established mathematical model is put in dimensionless form. The energy conservation equation is solved

for the three zones of the heat exchanger, i.e. fluid 1, fluid 2 and the wallseparating these two fluids, using a finite volume discretization method. The influence of the Peclet number of flows 1 and 2 on the spatial evolution of the dimensional mean temperature and the local Nusselt number is given:

- The effects of axial heat diffusion disappear for values of Peclet number greater than or equal to 50 (Peclet numbers being the same for both flows).
- For Peclet numbers below 50, the axial heat diffusion considered in our mathematical model becomes preponderant and its effect increases as Pe decreases.
- Axial heat conduction in hot and cold fluids leads to unfavourable heat exchange conditions in heat exchangers if they are used in energy recovery systems (e.g. heatingof a fluid). However, the use of these devices in cooling systems can improve their energy performance.

Bekkouche Mohammed Ismail, Trari Mansour [20], treated the dynamic and thermal behavior of a turbulent forced convection flow using the K-w model for two different thermal boundary conditions (heat flux, temperature), used to improve the performance of two-tube coaxial heat exchangers. This study allowed the authors to conclude that an increase of the velocity at the inner tube inlet near the rounded part of the exchanger is observed and which is generated first of all by the presence of recirculation zones resultingfrom an abrupt change in the direction of air flow.

An inverse proportionality between the evolution of the axial velocity of the flow and the temperature distribution in each cross section, the use of high Reynolds number values

Reynolds number, thus of high speed improves significantly the rate of friction and the rate of heat coefficient of friction and the rate of heat transfer.

1.6 Conclusion

A detailed description of heat exchangers has been presented throughout this chapter. All the constituent parts of this device have been discussed from a technological and functional point of view.

Chapter II: Theoretical Background

2.1. Introduction

Energy is an important input for social and economic development, due to their consumption activities in agriculture, industry and household energy demand has increased significantly. In terms of quantity, Brazil's domestic energy supply (DES) in 2010 reached 267.4 million oil equivalents (above), equivalent to 2% of global demand, of which 45.3% corresponds to renewable energy, while only 4% of this percentage From wind energy and solar energy [1], that is, solar energy is underutilized in Brazil. On the other hand, Germany uses solar energy extensively; despite its solar potential .On average the potential is 6 times lower than that of Brazil.

2.2. The Curie Circle

The name of the Curie wheel comes from its operating principle which it basically consists of heating and cooling a ferromagnetic material around its Curie temperature, Tc. Due to the heating of the material, a temperature gradient and an induced magnetic field are set takes different values along the length of the material, that is, it will be portions of material where it will be ferromagnetic and portions where will be the paramagnetic configuration of the a magnetic gradient in the armature as shown in **(Figure 1.1)**, where the arrows represent magnetic orientation for each part of the material [21]. When an external permanent magnet interacts with a magnetic gradient, the system is subject to magnetic forces, called driving forces, which will displace the rotor as shown in **(Figure 1.1)**.

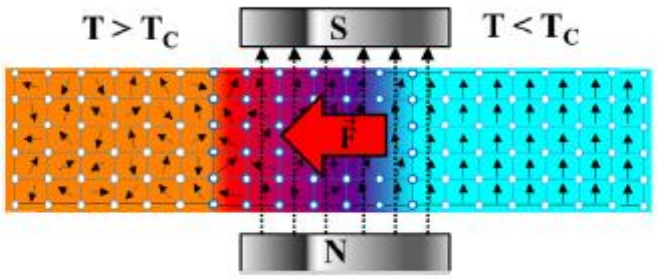

Figure 2.1. curie wheel working principal

2.3. Principle of operation of the curie motor

The principle of operation of the Curie motor is shown in **(Figure 2.1);** the exciting magnetic field is obtained by a stationary permanent magnet and in order to create a torque, one part the rotor is heated and the other part is cooled. If the warm side of the armature is heated above the Curie temperature, then, behaves magnetically like air or a vacuum.

Thus, the magnetic field energy density on the hot side increases and the permeability decreases; on the contrary, on the cold side of the armature, the energy density remains low and the magnetic permeability remains high. As a result, torque is generated and the rotor can start to move. Under these conditions, the Curie motor functions as a conventional magnetic device. In reality, however, the Curie engine will not produce a sharp interface between the hot and cold sides. However, in the region of the Curie temperature, a sharp difference in the magnetic properties of the rotor is induced. This effect allows the definition of a rotor line in which phase transitions take place. This line is called the phase transition line.

2.4. The DQ axis of the curie engine

The application of the DQ axis theory of electrical machines to describe the Curie motor encounters a fundamental difficulty: in the Curie motor, neither current are involved. As a result, you might think that the DQ theory does not apply to the Curie engine. However, in [22] showing how this difficulty can be overcome by comparing the field distribution of the Curie motor with that of the DC field machine. As mentioned above, the set of dynamic equations describing the Curie motor under steady-state conditions and assuming a constant excitation field is as follows:

$$\varphi = kI_d = const \qquad (1a)$$

$$C = M_{dq} I_d I_q \qquad (1b)$$

$$V_q = R_q I_q + \omega M_{dq} I_d \qquad (1c)$$

where φ is excitation flux, k is constant, I_d is sham the current along the direct axis that is capable of generating the excitation flux, V_q is a notional voltage on the quadrature axis

circuit, R_q is the dummy armature resistance, I_q is a fictitious current along the describing quadrature axis the magnetic poles needed to generate the field distribution induced by the temperature gradient, x is rotation velocity, M_{dq} describes the magnetic coupling between d and q axis, and c is the electromagnetic moment. Physical the importance of the electrical quantities used in the equations (1a) - (1c) explained in [22] and is briefly referenced below. Equation (1a) describes the excitation flux; due the fact that the excitation is generated by a permanent magnet, equation (1) is absolutely identical to the equation used for describe the excitation of a traditional DC machine and no in this case it is new.

As a result, I_d is a fiction the current that describes the excitation flux i, first approximation is constant and does not depend on the armature temperature. Equation (1b) describes the torque generated by Curie engine and includes news related to the description Curie engine. Torque is generated in the Curie engine by the difference in permeability between heat and cold dots. As already mentioned, I_d describes the excitation and therefore I_q is related to the permeability difference caused by temperature gradient. While at a standstill, T_h and T_c are regulated by convection heat exchange with cooling and heating systems and thermal conductivity between hot ones and cold spots inside the impeller. Using lumped parameters the temperature difference can be expressed as follows:

$$T_c - T_h = \frac{L}{kS} \cdot \frac{dq}{dt} \qquad (2)$$

Where T_c is the cold point temperature, T_h is the temperature in a hot spot, L is the distance, k is the thermal conductivity, S is the surface normal to the heat flow and (dq / dt) is the rate of heat. When parked, heat flows from a hot spot to a cold point and a constant temperature gradient is established. Maximum and minimum temperatures, T_h i T_c can be adjusted by adjusting the applied heating rate by the temperature of cooling and heating fluids. These they dictate temperatures (through their magnetic properties material) permeability difference, and therefore determine I_q.

If we assume that T_h and T_c are respectively above and below the Curie temperature of the material i this difference in permeability around the ferromagnetic critical the point is proportional to the power of this temperature difference, I_q can be expressed as follows:

$$I_q = k_1 \Delta T^{\omega} = k_1 \left(\frac{L}{kS}\frac{dq}{dt}\right)^{v} \qquad (3)$$

Where υ is the exponent describing the relationship permeability difference at the temperature difference and k_1 is a constant that allows you to match a focused parameter to actual values. If equation (3) is compared with equation (1c), you can: see that the voltage in the theory dq is played by the speed of heat (at a non-linear way if υ different from 1) If equation (3) is used to express w I_q in (1b), we get:

$$C = \frac{M_{dq}\, k_1 L^{v}}{k^{v} S^{v}} I_d \cdot \left(\frac{dq}{dt}\right)^{v} \qquad (4)$$

If the rotor is moving, a physical phenomenon is involved does not remain the same, but should also be considered advection (change in heat energy of a mass when moves in space). As a result, it can be shown that the temperature difference can be roughly expressed (at least in possible regimes for the Curie engine) as:

$$\Delta T = k_2 e^{-d\omega} \qquad (5)$$

Where d is the distance between the hot and cold points and x is the angular velocity, k_2 is the angular constant it takes take into account geometric details. [22] shows how this mathematical model is able to describe the experimental results published by other authors.

The analysis above presented clearly shows that the quantities that can be experimentally measured are: torque, rotational speed, heat rate, and applied magnetization[23].

2..3.1. A little history

The discovery of magnetism is traditionally attributed to Thales of Millet who, according to legend, noticed that his walk was slowed by the attraction of the nails of his sandals on a volcanic rock. The phenomenon may have been known before, but it was from this time (around 585 BC) that magnetite became known as a magnet stone. Until the 19th century, knowledge of magnetism only progressed very occasionally [24].

In the 6th century, the anti-Aristotelian John Philopon of Alexandria noticed the phenomenon of attraction and repulsion of magnets. Around the 9th century, the Chinese Shen Kua became interested in the magnet stone and mentioned the magnetization of a steel needle by the influence of a natural magnet. The alignment of the magnet towards the south is known in the tenth century but it is not excluded that the Arabs were the first to have exploited the phenomenon for navigation from the middle of the eleventh century: this would explain why Chu Yu mentions the introduction of the compass by foreigners in 10861. Finally, the compass was known in its present form in Europe in the early 12th century. The first real experimentation was carried out by Pierre de Maricourt in 1269 who defined the notion that William Gilbert would call in his work De Magnete in 1600, magnetic poles (by analogy with terrestrial magnetism). Gilbert's drawing (Fig I.3.1) shows the positions of the compass around a bar magnet. The quality of the experimental description is exceptional for the time.

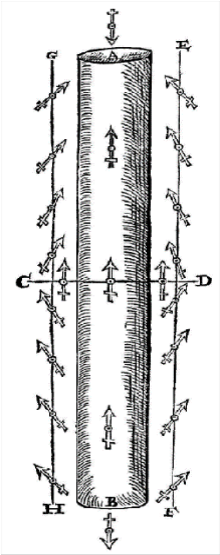

Fig 2.3.1: Positions of the compass around a bar magnet, source De Magnete by W. Gilbert

1.Some Chinese historical texts date the discovery of the compass to an earlier date, but the texts are more recent and certainly disingenuous.

Until the 19th century, the magnetism of materials remained an occult virtue supposedly at the origin of the most far-fetched phenomena, ranging from curative virtues to the revelation of adulterous women! Throughout this period, Descartes was the only one in 1644 to reject occultism and to propose a mechanistic interpretation, admittedly erroneous, but at least reasoned in light of the knowledge of the time.

The explosion of the science of magnetism took place in 1819 with the fortuitous discovery of the action of electric current on the deviation of the compass by Christian Oersted. Learning of the experiment, André Marie Ampère in 1820, suddenly became fascinated by this phenomenon. Although he had not been concerned with physics until then, he founded the theory of electrodynamics in four months. In 1827, he put forward the hypothesis that magnets were the seat of molecular currents (the atom was not yet known) which produced the magnetic field. Scientists from all over the world took up this theory and electrodynamics made great strides forward, thanks in particular to Jean Baptiste Biot, Félix Savart, Joseph Henry, François Arago, William Sturgeon, Perter Barlow...

It was at this time that Michael Faraday, a simple bookbinder's worker, became Humprey Davy's assistant. In 1821 he discovered the principle of the electric motor and induction in 1831. In 1845 he became interested in the magnetism of matter and distinguished ferromagnetism, paramagnetism and diamagnetism. He showed in 1852 that iron heated to red loses its magnetism. While Maxwell formalized the laws of electromagnetism in 1872, knowledge of materials progressed little until the beginning of industrial electricity.

In 1882, J.A. Ewing gave new impetus to magnetism by discovering hysteresis and then publishing in 1891 a complete work on the knowledge of the magnetism of matter (containing numerous measurements of magnetization as a function of field and temperature), after which he left to study earthquakes in Japan, where he founded the Japanese school of magnetism. In 1885, Hopkinson invented the chromium steel magnet, which was more coercive than magnetite and hardened steel, and in 1887, Lord Rayleigh established the first behavioural model of permeability as a function of field.

In 1895, Pierre Curie brought back the leadership of magnetism on our side of the Channel thanks to his work on the magnetism of pure bodies. He showed that diamagnetism is independent of the

temperature and established that the susceptibility of paramagnetics follows an inverse law of temperature, χ=C/T (Curie's Law). He measured very precisely the temperature at which ferromagnetism disappears (Curie's point) for various known magnetic materials (iron, nickel, magnetite...) but completely missed the law χ=C/(T-T_C) for ferromagnetics, which Pierre Weiss would only state in 1904. The same year, Paul Langevin exposed the theory of diamagnetism and paramagnetism, then in 1906, Weiss invented the molecular field and postulated the existence of magnetic domains. These two ideas were verified by the theoretical developments of Brillouin in 1927, Heisenberg in 1928 and Bitter's experiments in 1931, which made it possible to visualize the domains. During this time, materials were developed by Hadfield who invented iron-silicon (1900), Weiss (Fe2Co at 2.45 T, 1912), Elmen (permalloy, 1913), Honda (hard steel Co-W-Cr, 1917).

Finally, the 1930s saw the beginning of a constant progression in the performance of known materials and in the number of inventions, including: Alnico (Mishima, 1931), Cobalt-Platinum (Jellinghaus, 1936), soft ferrites (Snoek, 1933-45), hard ferrites (1952), amorphous (Duwez, 1960), SmCo magnets (1966), NdFeB (1980), and finally nano-crystalline (1988).

3.2. Phenomenology of magnetism

3.2.1. Hysteresis cycle, definitions

The first magnetization curve (Fig 2.3.2), corresponds to the evolution of B (induction) or J (polarization) as a function of H increasing from the demagnetized state (J=0, H=0). This curve is not reversible. For very small field strengths (typically less than 1 A/m for soft materials), the polarization depends linearly on the field [26].

$$J = \chi\mu_0 H \text{ as } B = J + \mu_0 H$$

We find

$$B = (1 + \chi_i)\mu_0 H = \mu_0\mu_i H$$

where χ_i (μ_i) is the initial susceptibility (relative permeability).

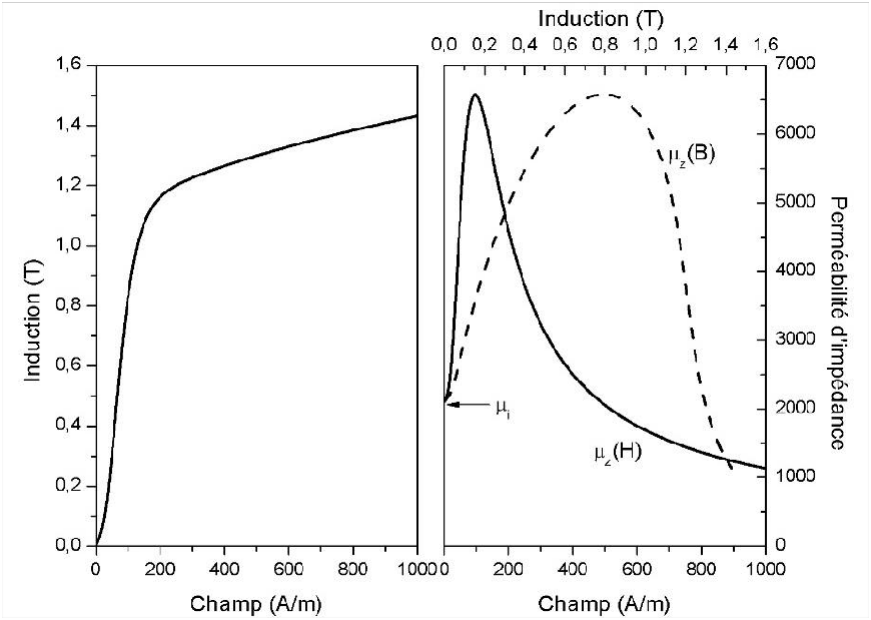

Fig 2.3.2: Typical first magnetization curve of a soft material (right) and variation of the impedance permeability with field (solid line) and induction (dashed line).

For larger values of H, this linear relationship no longer exists and the permeability is therefore no longer defined. To simplify the calculations, we linearize :

$$\mu_z = \frac{B_{max}}{\mu_0 H_{max}}$$

where μz is called the (relative) impedance or amplitude permeability. It corresponds to the value used to model magnetic circuits supplied with sinusoidal alternating current and depends on the amplitude of B (or H, see Fig 2.3.2).

When the material is saturated, we can write the induction

$$B = J + \mu_0 H = \mu_0 \mu_z H \qquad \Longrightarrow \qquad \mu_z = 1 + \frac{J_s}{\mu_0 H}$$

The energy that must be supplied to the material to reach a polarization point from the demagnetized state is called the magnetization energy (or sometimes work) density, WA. Since dWA=HdB, H>0 and dB>0, then WA>0. If we decrease the magnetic field until it is cancelled, the return branch does not follow the same path. Since dB<0, part of the energy is returned to the source and the rest is dissipated by Joule effect via various phenomena depending on the nature of the material.

If an alternating field is applied to the material, a cycle in the (H,B) or (H,J) plane, called the hysteresis cycle, is completed after one period. This cycle is traversed in the trigonometric direction. The area of this cycle corresponds to the volume energy dissipated in the form of heat during a cycle. The shape of the cycle depends on the chemical and structural nature of the material [26].

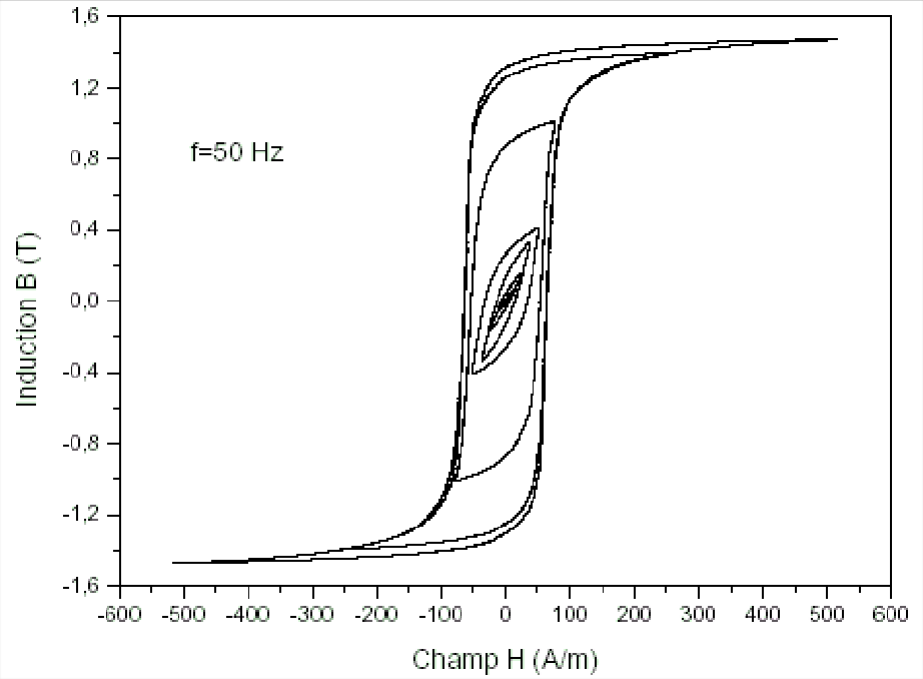

Fig 2.3.3: Major hysteresis cycle and minor cycles of a 3% FeSi sheet with non-oriented grains.

3.2.2. Soft-hard distinction

The characteristic quantities of a hysteresis cycle are as follows:

J_S: saturation polarization
J_R: remanent polarization (H=0 starting from the saturated state)

H_{CJ} : coercive field (J=0 starting from the saturated state)

H_K : anisotropy field (when $J=J_S$)

In the plane (H, B) we can define

$B_R = J_R$ the remanent induction (because at this point H=0)

H_{CB} : coercive field (B=0 starting from the saturated state)

It should be noted that the term "saturation induction" has no physical meaning insofar as

$$B=J_S+ \mu_0 H \quad \text{if} \quad H \rightarrow \infty$$

The distinction between soft and hard is made by the coercive field.

- $H_{CJ}<100$ A/m, the material is soft: it is magnetizable and spontaneously demagnetizes
- $10^4<H_{CJ}<2.10^6$ A/m, the material is hard: if it is magnetized it remains so permanently
- $100<H_{CJ}<10^4$ A/m, the material is said to be semi-hard

For a soft material, JS is of the order of a tesla and saturation is reached for a field of the order of H=8000 A/m, hence :

$$B=J_S+ \mu_0 H \sim 1+ 4.10^{-7} \sim 1.01 \text{ T}$$

i.e. a difference of about 1% between polarization and induction, which explains the misuse of the term saturation induction for soft materials.

For a magnet under a field at $H=H_{CJ}$~800kA/m

$$B=J_S+ \mu_0 \mu_i H_{CJ} \sim 1+4.10^{-7} 10^5 \sim 2 \text{ T}$$

In this case it is essential to differentiate between the notions of polarization and induction, as can be seen in Fig I.3.4, where we also see that $H_{CB}<H_{CJ}$. For a very good magnet, $H_{CJ}>\mu_0 B_R$ which implies that $H_{CB}=\mu_0 B_R$.

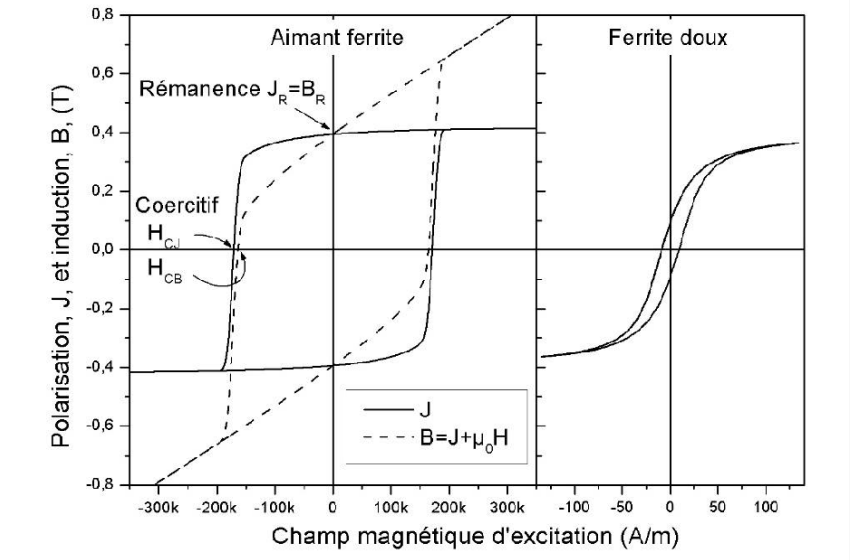

Fig 2.3.4: Example of hysteresis cycle for hard and soft ferrite

3.2.3. Domain structure

Paramagnetic and ferromagnetic elements all carry a magnetic moment, but in the first case they are thermally excited, so that the polarization is zero in the absence of a field and very weak at usual temperatures and fields. In the second case, the exchange energy, which is linked to the exchange of electrons between the atoms, tends to orient all the moments [25].

These moments orient themselves towards the direction of easy magnetization (a particular direction of the crystal). These moments orient themselves towards the direction of easy magnetization (a particular direction of the crystal). This situation gives rise to significant magnetostatic energy. The system tends to minimize the magnetostatic energy by creating zones of opposite magnetization. When passing from one area to the other, the Bloch wall, the magnetization turns 180° in a helix. The energy associated with the wall depends on the magneto-crystalline anisotropy constant (which tends to align the magnetic moments in a particular crystallographic direction) and the exchange constant. Depending on the magnitude of these terms, a finite number of walls are created in each grain. The Bloch walls have a width of the order of 5 nm (~15 atoms) for hard and 100 nm for soft (~300 atoms). If the anisotropy energy is small, the material is demagnetized in the absence of a field and magnetization occurs by wall displacement and moment rotation (see Fig I.3.5).
If the anisotropy energy is strong, the walls are thin and easily trapped by the defects of the crystal and the influence of the magnetostatic energy is weak. After magnetization, the moments remain locked along the axis of easy magnetization and we have a magnet [25].

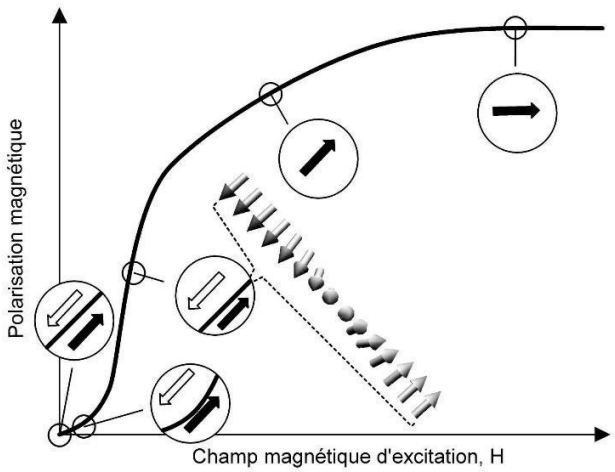

Fig 2.3.5: Evolution of the domain structure as a function of the field for a soft magnetic material. The zoom shows the structure of the wall.

3.3. Crystalline metallic materials

3.3.1. Pure magnetic metals

There are only three elements that carry a strong magnetic moment at room temperature: iron, cobalt and nickel. Of these three elements, iron has the highest magnetic moment, Js=2.16 T at 300 K, and is by far the most abundant and therefore the least expensive. Pure iron is rarely used because its hardness and elasticity are poor, it cannot be finely rolled, it is susceptible to corrosion and its resistivity is low. Pure iron is therefore only used in massive form and under continuous magnetic field (large electromagnets).

Pure cobalt is not used because it is not really soft or hard enough and nickel has too low a polarization to be interesting (Js=0.6 T at 300 K).

3.3.2. Iron-silicon alloys.

In the early history of electricity, metallurgists sought to obtain the purest iron possible to improve these magnetic qualities. In fact, it was mainly a question of eliminating the carbon responsible for the precipitation of hard phases in steels (notably martensite). In 1896, Hadfield discovered that the fortuitous presence of a few percent of silicon in iron improved its mechanical qualities, but he did not study its electromagnetic properties until 1900.

The presence of silicon at a rate of 2 to 4% of the mass confers to the alloy a strong increase in hardness and yield strength, a clear improvement in laminability, a better resistance to corrosion, a multiplication of resistivity by 4 and an anisotropy divided by 2 for a loss of polarization to saturation of less than 10% [25].

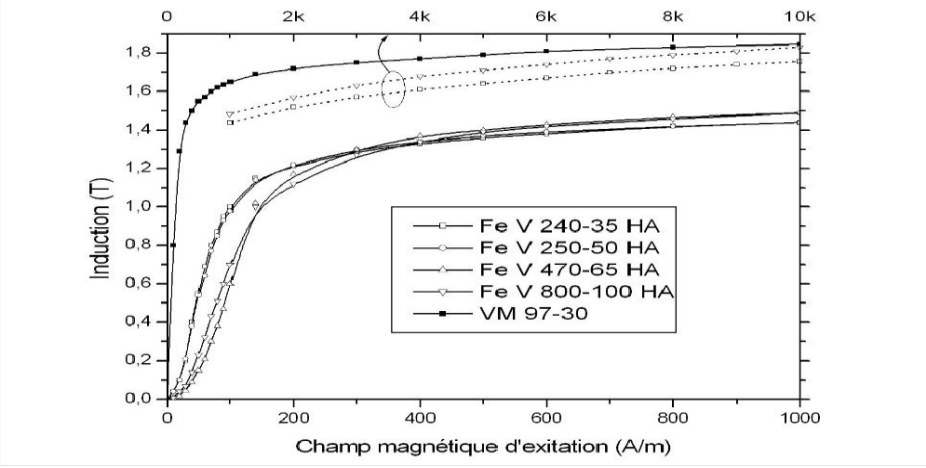

Fig 2.3.6: Magnetization curves for 4 types of NO laminations compared with a conventional GO. It can be seen that all curves converge towards 1.8 T but for fields that differ by an order of magnitude between NO and GO. For NO laminations, the permeability at low field increases with the thickness.

There are two families of Fe-Si sheets.

Non-grain oriented sheets, NO, are essentially isotropic in the plane and grain oriented sheets, GO, are anisotropic in the rolling axis.

NO plates are produced by hot rolling (1000-13000°C) and cold rolling (300-40°C) to 40-60/100 mm followed by annealing (800°C). The so-called "semi-process" sheets are then insulated and cut. The so-called "full process" plates are usually cold worked to 35/100 mm, cut, annealed and insulated.

GO plates are hot rolled once and cold rolled twice and then annealed. They are treated with magnesia before undergoing a recrystallization annealing process which will promote the growth of crystals along the rolling axis and will allow to obtain the Goss crystallographic texture, named after its inventor (GOSS also means grain oriented steel sheet, it can't be invented!) GO plates, known as HiB (pronounced "aïe bi"), undergo a more advanced process that increases the size of the grains and improves the orientation. At the same time the thickness is increased to 20, 10 or even 5/100. In addition, a special coating is used to apply a permanent tensile stress which increases permeability and reduces losses [25].

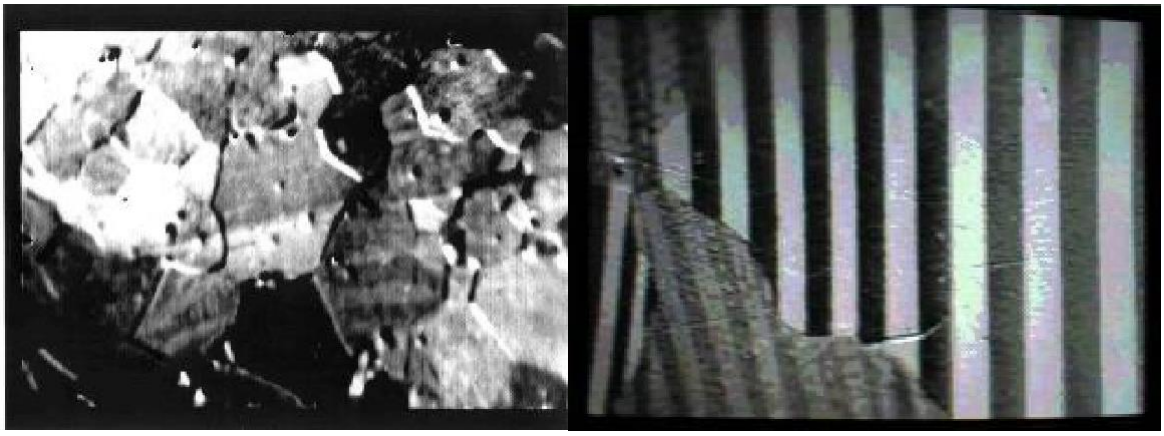

Fig 2.3.7: Domain structures visualized by magneto-optical Kerr effect (width of the images 3mm). In the NO laminations the orientation and size of the domains is very variable (left). GO laminations have much larger grains and wide domains (right).

In Fig I.3.6, we can see that the induction in the GOs rises very quickly to a value close to saturation. This can be explained very well when we look at the domain structure in Figure 2.3.7: the domains are large and well aligned along the rolling direction (LD). When the field is applied along this axis, the domains move easily and the rotation process is almost absent. For the NWs, we see that the wall displacement process is completed around

200 A/m (as for GOs). On the other hand, since the domains are misaligned, it takes a lot of energy to rotate all the magnetic moments in the direction of the field.

GO laminations are used in transformers or chokes. For transformers above 1 kVA, they can be cut into E-I, knowing that the field in the E columns and the I must be //DL. In the E yoke, the field is transverse to the DL, so the losses are higher in this area (about 4 times). Transformers over 10 kVA are made from assembled I's (the connections are cut at 45°). It is also possible to make toroidal or rectangular wound magnetic circuits from 100 to 50 µm GO laminations (in this case they are cut in two to pass the windings). NO laminations are reserved for small transformers (because of the price) and rotating machines.

The steel standard classifies FeSi plates with respect to losses and thickness as :

M - 000 - 00 X

The M stands for magnetic, the first digit indicates the losses expressed in W/kg 100 measured at 50 Hz 1.5 T (1.7 T for S or P), the second digit indicates the thickness expressed in 100th of mm and the final letter the quality (A, D or E for NO, N, S or P for GO)

3.3.2Iron-cobalt alloys

After Weiss' work on FeCo, G.W. Elmen showed in 1926 that the alloy containing 50% of each metal was much more permeable with approximately equal polarization (2.4 T). However, as this material is difficult to roll, additions are necessary. The most common industrial alloy is Fe48Co48V2 because the vanadium, in addition to improving the laminability, increases the resistivity of the alloy from 6.3 to 26 µcm. This material is reserved for military and aeronautical applications because cobalt is an expensive and strategic metal (39% of the world resource in Zaire, 30 in Cuba, 10 in Zambia, 7 in New Caledonia). The current trend is to reduce the percentage of cobalt to 25 or 18% by improving the orientation of the grains to preserve the magnetic softness [26].

3.3.3. Iron-nickel alloy

The first Fe-Ni alloys were studied by Hopkinson in 1889, but it was not until 1921 that an alloy containing 78% nickel (Permalloy 78) found application as a magnetic material in telephony.

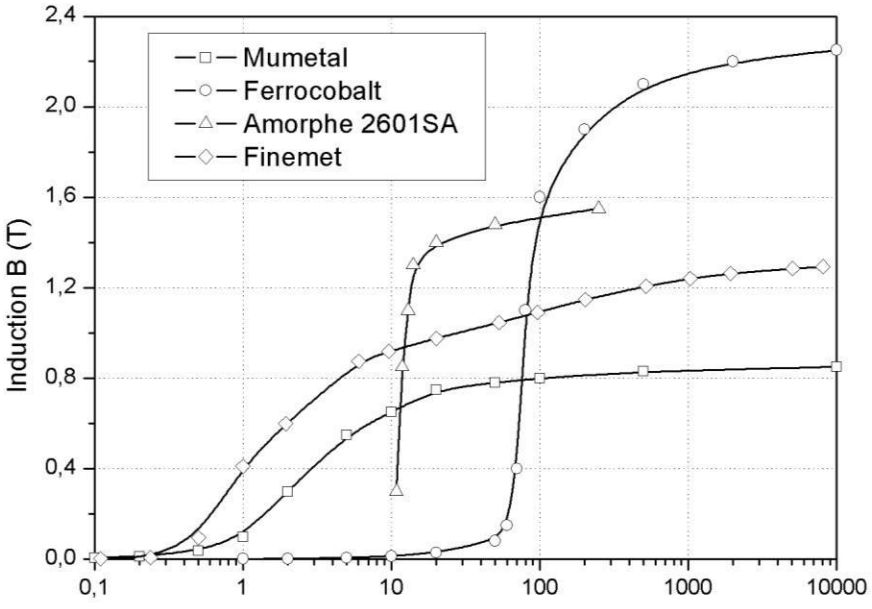

Fig 2.3.8: First magnetization curves of different crystalline and amorphous special alloys [26].

Fe-Ni alloys are high permeability alloys. They are mainly divided into two families:

- Permalloy 50, Ni50Fe50, high bias (1.6 T)
- Permalloy 80, Ni80Fe20, with high permeability (~90,000) and low polarization (0.8 T).

Many grades of Permalloy 80 are available containing additive elements whose role is to slightly modify certain physical parameters in order to obtain, for example, zero magnetostriction2 and zero anisotropy at the same time and to increase the resistivity. The main commercial alloys are

- Mollypermalloy, Fe15Ni80Mo5 with optimum resistivity and permeability, which is also used in the form of bonded powders for circuits with a distributed air gap (permeability 20 to 300) which can be used at high frequencies thanks to their fine grain size (20 to 100 µm).
- Mumetal, Fe13Ni78Mo4Cu5 or Fe16Ni77Cr2Cu5, with lower performances but much easier to manufacture (therefore cheaper).

Magnetic FeNiCr stainless steel is also used for induction tableware. The composition allows the Curie point to be adjusted to the desired temperature, thus allowing natural regulation of the cooking temperature.

These alloys are intended for specific applications where very high permeability is essential. Nickel is less strategic than cobalt because resources are more abundant and better distributed [25].

2.4 Conclusion

A detailed description of the curie engine has been presented throughout this chapter. All the constituent parts of this engine have been discussed from a technological and functional point of view.
and functional point of view. Finally, general information on magnetism

2 Magnetostriction is a phenomenon of deformation of material under the action of a magnetic field. The opposite phenomenon can be used to make force transducers, but it is often considered harmful because a stress applied to the magnetic circuit can lead to a degradation of the magnetic properties.

Chapter III:
Optimisation of curie motor

3.1. Introduction

Experimental validation of the CFD results

In order to assure the results produced by the CFD simulations were consistent with reality, a series of validation experiments were done. The experiments aim to emulate the heating conditions that are going to be applied to the heat exchangers used in the thermomagnetic motors. Therefore, two plates, one of SAE 1020 steel and the other of aluminum alloy 6061 were built, with dimensions and geometry as shown in Fig. 1 and a total heat transfer area of 7122.44 mm^2. The plates were heated by a water flow through the internal channels, emulating the real conditions that will be used in the operation of a thermomagnetic motor prototype. The mass flow rate through the plate which was used in the experiment was 0.025 kg s^{-1} heated to a temperature of 343.15 K. The plate was initially at room temperature (around 298 K), and its temperature was taken using a type K thermocouple fixed to the center of the upper area of the plate, the sensor signal was amplified and sent to a data acquisition software which registered the temperature of the plate as a function of time. The experiment was realized three times for each plate [28].

The CFD simulation parameters were then chosen in accordance with real world conditions, i.e., the same mass flow rate, temperatures, geometry, initial conditions for the plate and a simulation time equal to the heating time measured in the experiments (with a time step of 0.1 s). In order to guarantee compatibility between the experiments and the simulation results, the properties of the selected materials are presented in Table 1 and these properties were the ones used in the CFD software [29].

Except for extremely viscous fluid flow in pipes of small diameter, the fluid flow can be considered turbulent (Fox et al., 2004). The Reynolds number determined by the CFD simulations for the plate geometry shown in Fig. 1 was 3172.0, which implies that the fluid flow in our experiment is turbulent.

	SAE 1020 steel	Aluminum alloy 6061
Molar mass (kg kmol^{-1})	58.55	**26.15**
Density (kg m^{-3})	7850	**2700**
Specific heat capacity(J kg^{-1} K^{-1})	486	**896**
Thermal conductivity(W m^{-1} K^{-1})	51.9	**180**
Thermal expansivity (K^{-1})	**11.7e—6**	**23.6e—6**

Table 3.1 Material properties used in the simulation (Callister, 2000).

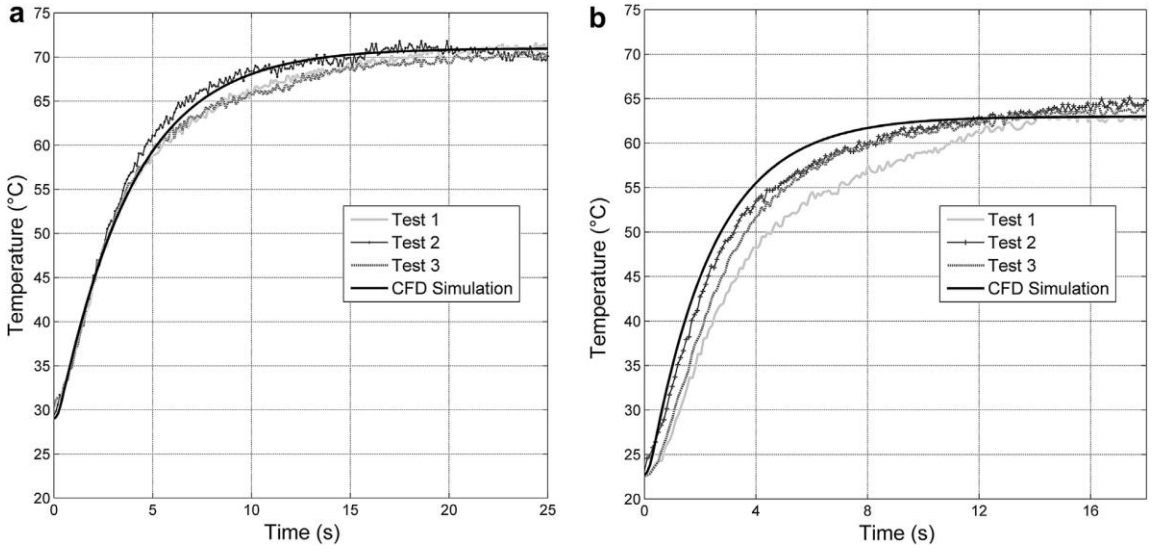

Figure 3.1 Comparison between the experimental and simulation data for the test plates: a) SAE 1020 steel; b) aluminum alloy 6061.

As we declared in Chapter 1, the NaviereStokes equations do not produce results for all fluid flow processes, requiring models to be approximated to derive these additional equations [27]. One of the most important aspects to be solved with approximation models is the state of fluid flow turbulence, and in our simulations we used the ke3 model, which is the most widely used and validated turbulence model, and is also the simplest model for which only initial conditions and / or shoreline.

There are several options for specifying the amount of inlet turbulence. In the absence of more detailed experimental information on turbulence levels, the average intensity value shall be used. Nominal turbulence intensities range from 0.1% to 10%, which correspond to very low and very high levels of turbulence in the flow (ANSYS, 2010b) [27]. As no other information about the turbulent kinetic energy was available through experiments, a medium value of 5% intensity was assumed in the present work.

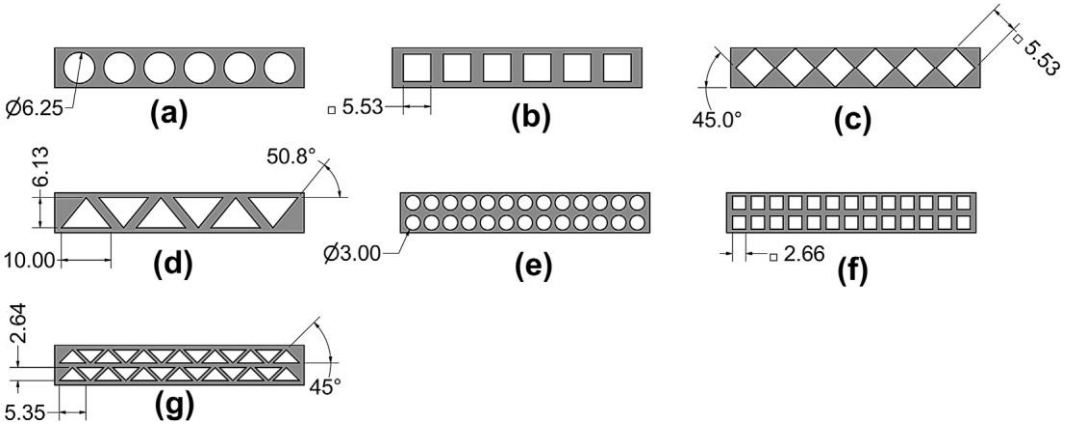

Figure 3.2. Simulated channels geometries: a) 6 circular channels; b) 6 square channels; c) 6 rotated square channels; d) 6 triangular channels; e) 26 circular channels; f) 26 square channels; g) 26 triangular channels [27].

Channel geometry	Total heat transfer area (mm^2)	Total hydraulic diameter (mm)
26 Circular channels	28 489	**79.00**
26 Square channels	31 765	**69.15**
26 Triangular channels	36 396	**57.48**
6 Triangular channels	17 890	**28.98**
6 Square channels	16 894	**34.19**
6 Rotated square channels	15 048	**33.88**
6 Circular channels	**13 383**	**37.47**

Table 3.2. Total heat transfer area and hydraulic diameterfor each channel geometry.

Figure 3.2 shows the results when the SAE 1020 steel was used as the plate material and (Figure 3.2) shows the results for the case in which the plate material was the 6061 aluminum alloy. These figures confirm that the experimental and simulated results agree satisfactorily, showing that the assumptions made for the simulations were consistent with reality and therefore validating the simulations [27]. The difference between the CFD simulation and the experimental data is larger in the case of the aluminum alloy plate; there were some experimental difficulties in fixating the thermocouple sensor to the plate, possibly causing this difference. Future experiments shall be made in order to acquire more reliable data.

3.2. **Study of the channels geometry**

In order to optimize the frequency and hence the power generated by the thermomagnetic motor, it is essential to accelerate the heat transfer rate in magnetic heat exchangers. To this end, the different channel geometries of the internal magnetic heat exchangers were simulated with the CFD software. Initially, seven different channel configurations were analyzed, with geometries and dimensions as shown in (Figure 3.3). In order to compare the results, all boards have the same external dimensions (8 × 50 × 110 mm) and the same material volume, regardless of the shape and size of the channels. Therefore, the geometry and arrangement of the internal channels are the only changing parameters of the plates [27]. In order to compare the difference between the channel geometries, the total heat transfer area and the total hydraulic diameter are shown in (Table 3.1). This is done because these two parameters have a strong influence on the heat exchangers transfer rate.

For these new simulations the same model parameters already validated were used, i.e., a mass flow rate of 0.025 kg s^{-1} of water heated to 343.15 K, with an inlet turbulence intensity (using the *k*e3 model) of 5%. The material selected for the plates was standard steel, i.e., density of 7854 kg m^{-3}, molar mass of 55.85 kg mol^{-1}, specific heat capacity of 434 J kg^{-1} K^{-1} and thermal conductivity of 60.5 W m^{-1} K^{-1}. As the main objective of these simulations is to compare the heat transfer rates for different geometries of the magnetic heat exchanger channels, the use of the properties of the actual thermomagnetic materials in the simulations is not fundamental. The simulation total time used was 30 s with time steps of 0.5 s.

The average plate temperatures as a function of time are shown in (Figure 3.4).

The contact area between the fluid and the plate inside the channel is defined by both the perimeter of the channel and the length of the plate. The graphs in (Figure 3.4) show that the larger the contact area, the higher the heat transfer, despite the reduction in the hydraulic diameter. The use of more channels (with a constant volume of material in the plate) results in a larger contact area and thus a better heat transfer rate[27]. Also, the orientation of the channels does not significantly affect the average plate temperature, as seen in the comparison between a plate with six square channels and a plate with six square channels turned 45 ° with the same dimensions.

Another interesting conclusion arising from the analysis of these curves is that the average

temperature of the plates increases exponentially with time, once the temperature difference between the plate and the heating fluid is initially high and decreases steeply as the temperature of the plate converges to the temperature of the heating water. Based on this, we suggest that, in order to maximize the frequency of the motor.

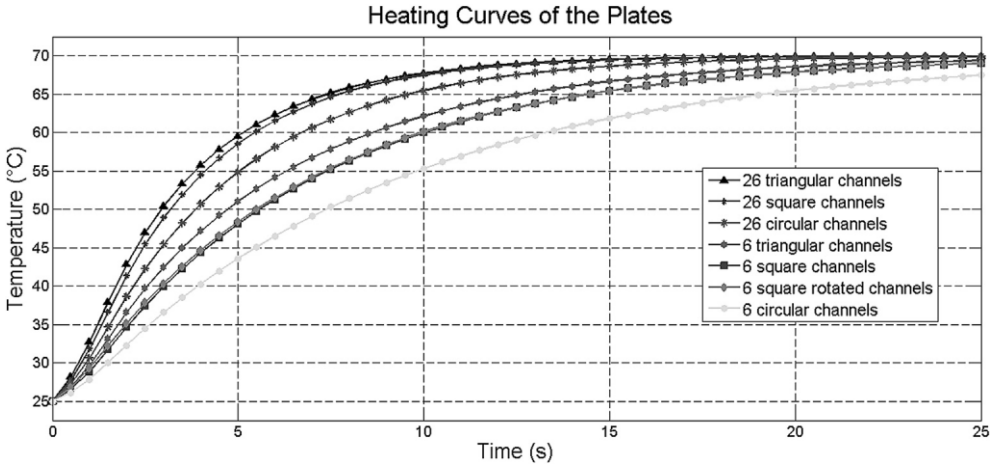

Figure 3.4. Comparison between the heating curves for different heat exchanger channel geometries.

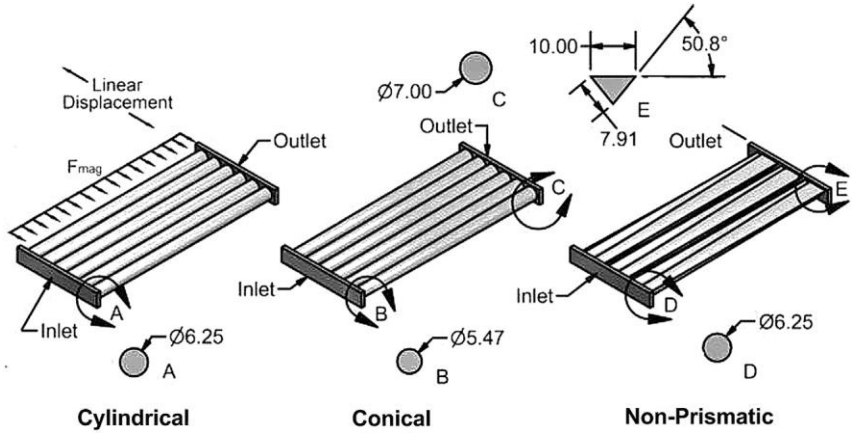

Figure 3.5. Channel's geometries aiming to reduce the temperature gradient along the length of the magnetic plate: a) cylindrical channel (for comparison); b) conical channels; c) non-uniform geometry channels

It is important for the engine to use a magnetocaloric material whose Curie temperature (Tc) value is close to that of the cold fluid being added with a 60% temperature difference between the hot and cold fluid temperature. For thermomagnetic motors to function properly, it is important that, if not all, at least most of the volume of the plate's magnetic material reaches the Curie temperature (Tc) at the same time. Therefore, the temperature gradient along the entire length of the slab must be kept to a minimum.

To improve this, we suggest that the channels have a variable cross-section along the length of the slab. To investigate this possibility, we selected two new configurations of internal channels as shown in Figure 3.5, the first is a conical channel with diameters ranging from 5.469 to 7mm (Figure 5b) and the second is a cross section varying from a circular shape at the inlet (diameter 6.25 mm) to triangular at the outlet (Fig. 5c). The simulation results for these two channel shapes were compared with the previous results for the cylindrical shape (Fig. 5a).

The main idea of these new designs is to vary the contact area along the length of the plate, from a smaller heat exchange area in the inlet (where the fluid is hotter and the highest temperature of the plate is expected) to a higher heat exchange area in the outlet. The conditions of the fluid and the plate (be- sides the channel geometries) are the same as in the previous analyses.

Fig. 6 presents the volume of the plates above the defined Curie temperature (318 K) as a function of time, i.e. the volume of the plates that has changed its magnetic behavior.

The closer the heating curve is to the tier function, the better the temperature distribution in the plate. It appears that the discontinuity in the behavior of the curve for channels with a non-constant section between 4.5 and 6 s is mainly due to the geometric transition factor adopted in the channel design (see Figure 5c), as this causes the center area of the plate to have a lower velocity heat exchange than the end area of the plate. Thanks to these analyzes, we can see that channels with a non-constant cross-section (as can be seen in Fig. 5b and c) not only provide a more uniform temperature distribution along the length of the plate, but also a better heat transfer rate than cylindrical channels. While these formats can present challenges to magnetic plate manufacturing processes, knowledge of these alternatives can lead to better magnetic heat exchangers for thermomagnetic-motors.

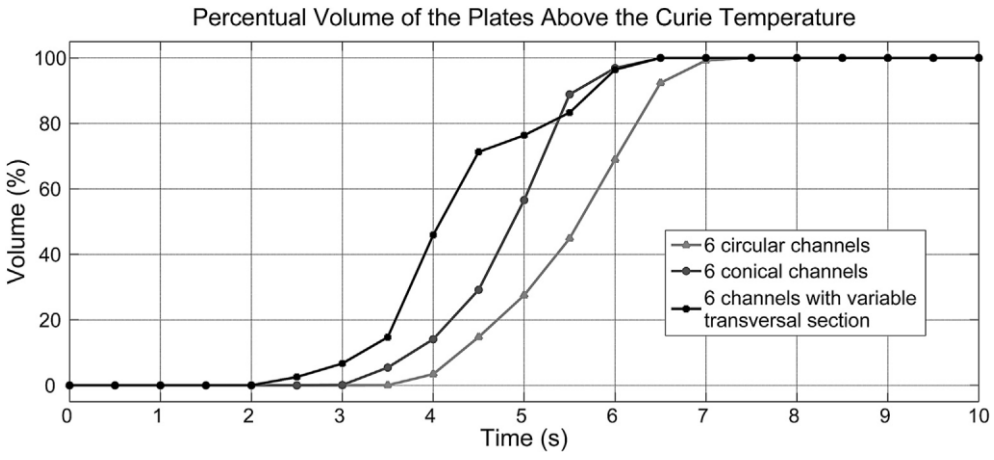

Figure 3.6. Volume of the plates above the Curie temperature as a function of time.

3.3. Conclusion:

This chapter presents an approach to the optimization of the Curie engine. Approach is based on a dynamic model of a thermomagnetically coupled engine, which is obtained by assuming: the use of a ferromagnetic material operating at temperatures close to the Curie point analytical an expression of the generated torque which combines this quantity with magnetic, thermal and geometric the parameters of the generated torque are given. Expressions of speed and torque were derived and related to the thermal properties of the machine and are used as optimization indicators in optimization procedure. The goal of the optimization process is to obtain a machine capable of continuous rotation at maximum achievable power. A machine design based on this theory is proposed and the associated performance is simulated numerically. Initial experimental verification performances are reported.

General conclusion

General conclusion

This work explored the optimization procedures of heat ex- changers to be used in thermomagnetic motors. The article main focus is the use of CFD simulations to maximize the heat exchange rate between the magnetic materials and the hot and cold fluids. This is done in order to have the maximum possible operational frequency in thermomagnetic motors. This was accomplished by optimizing the geometries of the channels of the heat exchangers.

As the focus of this work was to improve the thermo- magnetic heat exchangers geometrically, some important characteristics were observed. First of all, taking into account the fact that the heat transfer rate is highly influenced by the contact area between the fluid and the plate, and that the length of the plate is constant and depends on constructive characteristics of the motor, we have that, in order to improve the heat transfer speed, the perimeter of the channels must be increased. In this work only channels having convex cross section formats were considered, but the use of channels with concave cross section may lead to higher contact areas and therefore improve even more the heat transfer rate.

Another very important aspect is that the temperature gradient along the plate needs also to be taken into account, because the magnetic force distribution applied on the plates is perpendicular to its linear displacement, so this gradient can lead to some misalignment of the force on the plates leading to the blockage of the motor; in this sense we showed that the best option to maximize the temperature homogeneity is the use of a non-uniform cross section in the channels.

Future works shall be developed considering the real properties of the magneto-caloric materials for the simulations, which will allow the use of the CFD simulations together with magnetic simulations to determine the dynamics of thermomagnetic motors and also their efficiencies.

Bibliographical references

References:

[1].World Commission on Environment and Development (WCED), 1987. Report of the World Commission on Environment and Development: “Our Common Future” [S.l.]. United Nations <http://www.un-documents.net/wced-ocf.htm>. Xuan, Y., Lian, W., 2011. Electronic cooling using an automatic energy transport device based on thermomagnetic effect. Appl. Therm. Eng. 31, 1487e1494.

[2]. Gnielinski V (1976) New equations for heat transfer in turbulent pipe and channel flow. Int Chem Eng 16:359–368

[3]. Gnielinski V, Zukauskas A, Skrinska A (1983) Banks of plains and finned tubes, single phase convective heat transfer. In: Heat exchanger design handbook, vol 2, 2.5.3.1–2.5.3.16

[4]. Bougriou C (1991) Etude du transfert de chaleur par condensation d’air humide sur des tubes a` ailettes. PhD thesis, INSA de Lyon ISAL87

[5]. Gnielinski V (1978) Gleichungen zur Berechnung des warmeu¨- bergangs in querdurchstromten einzelnen rohrreihen und rohrbudeln, Forsch. Ingenieurwes 44:15–25

[6]. Zukauskas A, Ambrazyavizius AB (1961) Heat transfer of plate in a liquid flow. Int J Heat Mass Transf 3:305–309

[7]. Bouvenot A (1981) Transfert de chaleur. Masson, Paris

[8]. Sacadura JF (1980) Initiation aux transferts thermiques. Techniques et Documentation, France

[9]. Frass AP, Ozisik MN (1965) Heat exchangers design. Wiley, New York

[10]. Afgan V, Schlunder EU (1974) Heat exchangers; design and theory. McGraw-Hill, New York

[11]. Bougriou C, Baadache K (2008) Shell-and-double concentrictube heat exchangers. Patent PCT, DZ2008/000002

[12]. Bougriou C, Bessaı¨h R (2005) Determination of apparent heat transfer coefficient by condensation in an industrial finned-tube heat exchanger: prediction. Appl Therm Eng 25(11–12): 1579–1587

[13]. Bougriou C, Bessaı¨h R, Bontemps A (2005) Experimental and computational performances of heat exchangers functioning in wet regime by using the film method. Int Commun Heat Mass Transf 32:1135–1142

[14]. Bougriou C, Bessaı¨h R, Bontemps A (2005) Experimental study of performances of industrial heat exchangers functioning in wet regime. Int J Heat Exch 6:179–202

[15]. Bougriou C, Bessaı¨h R (2007) Prediction and measurement of apparent heat transfer coefficient by condensation in finned-tube heat exchangers. Heat Transf Eng 28:940–953

[16]. Bougriou C (2002) Etude du re´cupe´rateur de chaleur croise´ a` tubes a` ailettes. Revue des Energies Renouvelables 5:59–73

[17]. Bougriou C (1999) Etude du re´cupe´rateur de chaleur croise´ a` tubes lisses. Revue des Energies Renouvelables 2:109–122
[18]. Bougriou C (1998) Calcul et technologies des e´changeurs. Department of Mechanics, University of Batna, Batna
[19]. Baadache K (2005) Etude nume´rique d'une changeur de chaleur a` triple tube concentrique en re´gime permanent (Co-courant et Contre-courant). Department of Mechanics, University of Batna,
[20]. Sekulic DP, Herman CV (1987) Transient temperature fields in a three fluid heat exchanger. In: Proceedings of the 17th international congress of refrigeration, Vienna, B, pp 833–837
[21]. https://tel.archives-ouvertes.fr/tel-00352970/file/20061205_These_DUBAS_France.pdf
[22]. M. Trapanese, "A dq axis theory of the magnetic, thermal, and mechanical properties of Curie motor," J. Appl. Phys. 109, 07E706 (2010).
[23]. K. Murakami and M. Nemoto, "Some experiments and considerations on the behaviour of thermomagnetic motors," IEEE Trans. Magn. Mag. 8, 387–398 (1972).
[24]. De Magnete, W. Gilbert, 1600, https://www.lancaster.ac.uk/fass/projects/gilbert/docs/DeMag.pdf
[25].https://eduscol.education.fr/sti/sites/eduscol.education.fr.sti/files/ressources/pedagogiques/12884/12884-materiaux-magnetiques-doux-pour-la-conversion-denergie-ensps.pdf
[26]. Techniques de l'Ingénieur, articles in the materials section of the treatise Génie Electrique (D2 and D3).
[27]. www.sciencedirect.com/trapense2014
[28]. ANSYS, 2010a. ANSYS CFX Introduction. Ansys Inc, p. 60. Release 13.0-support material.
[29]. ANSYS, 2010b. ANSYS CFX Solver Modeling Guide. Ansys Inc, p. 486. Release 13.0-support material. Callister Jr., W.D., 2000. Material Science and Engineering: an Introduction. John Wiley & Sons, Inc., New York, p. 871.